



Full Length Article

Synthesis of 1-(4-chlorobenzoyl)-4-(dimethylamino) pyridin-1-ium chloride and determination of cytotoxicity and apoptosis in human colon cancer cells

Bader O. Almutairi^{a,*}, Saud M. Almutairi^{b,*}, Saud Alarifi^a^a Department of Zoology, College of Science, King Saud University, PO Box 2455, Riyadh 11451, Saudi Arabia^b King Abdulaziz City for Science and Technology, Riyadh 11442, P.O. Box 6086, Saudi Arabia

ARTICLE INFO

Keywords:

Cytotoxicity

Protein profiling array

Oxidative stress

HCT-116 cell

Caspase-3, caspase-8, p21, and p53 gene

expressions

ABSTRACT

Background: In this experiment, we synthesized a new compound, 1-(4-chlorobenzoyl)-4-(dimethylamino) pyridin-1-ium chloride (SM-9), and examined its toxicity and anticancer activity in human colon cancer (HCT-116) cells.

Methods: We uncovered the underlying mechanisms of cell toxicity and apoptosis due to SM-9 compound exposure in HCT-116 cells by using the MTT assay and protein profiling array and measuring gene expression levels using reverse transcription-polymerase chain reaction.

Results: Our data show that the SM-9 compound activated the caspase-3, caspase-8, p21, p27, and p53 proteins involved in the apoptosis of HCT-116 cells, thereby inducing cytotoxicity, the formation of reactive oxygen species, and apoptosis. The results of this study show that the SM-9 compound has advantageous qualities and must be taken as an anticancer medication. We conclude that the SM-9 compound exerted an anticancer effect by inducing the apoptotic pathways in human colon cancer (HCT-116) cells.

1. Introduction

Over the past 10 years, ionic liquids have drawn a lot of attention owing to their special qualities that may be useful for cutting-edge technologies and procedures. Ionic liquids include corrosion inhibitors (El-Hajjaji et al., 2019), antimicrobials (Albalawi et al., 2018; Titi et al., 2021), and antiviral and anticancer medicines (Titi et al., 2020). In this study, we created an ionic liquid (1-(4-chlorobenzoyl)-4-(dimethylamino) pyridin-1-ium chloride, the SM-9 compound, and tested its cytotoxicity and antioxidant qualities in human colon cancer (HCT-116) cells for 24 h. The toxicity of the SM-9 compound is caused by several processes, including increased generation of reactive oxygen species (ROS) in stressed live cells.

The mitochondria are the main source of ROS generation in tissues and most ROS produced in the chain of the electron transport system (Hansford et al., 1997). The electron is released from the chain of the electron transport system directly to oxygen, inducing the release of tiny-lived free radicals such as singlet oxygen and superoxide anions (Hansford et al., 1997). In this experiment, we synthesized a new chemical compound, SM-9, and investigated its toxic effects on human

colon cancer cells. Ali et al. (2023) reported that biosynthesized cobalt nanoparticles with garlic and onion peel inhibited bacterial growth. In addition, our findings are useful for determining the safety profile of synthesized compounds as raw materials for the manufacturing of anticancer drugs. 4-(Dimethylamino)pyridine is a cheap and ingenious chemical that induces skin toxicity. ROS creates cellular oxidative stress that leads to colon damage and colon cancer (Bardelčková et al., 2023), but at the cellular level, the natural defense system of the colon is damaged in response to chemical compounds. ROS severely deteriorates biomembranes and biomolecules and induces the expressions of matrix metalloproteinases (Tu and Quan, 2016).

Drug toxicity includes various mechanisms, mainly the generation of extra-ROS. Schumacker et al. (2014) and Almutairi et al. (2021) reported that mitochondrial damage is due to ROS overproduction in cells. Toxicity induced by contaminant and drug compounds in target cells is due to ROS production and apoptotic and inflammatory processes (El-Sayed et al., 2005). Oxidative stress mainly results from ROS generation. Overproduction of ROS induces the imbalance of the antioxidant mechanism in cells, which consequently leads to the peroxidation of lipid molecules and other oxidative-related stress enzymes (Su et al.,

* Corresponding authors.

E-mail addresses: bomotairi@ksu.edu.sa (B.O. Almutairi), salmutairi@kacst.edu.sa (S.M. Almutairi).

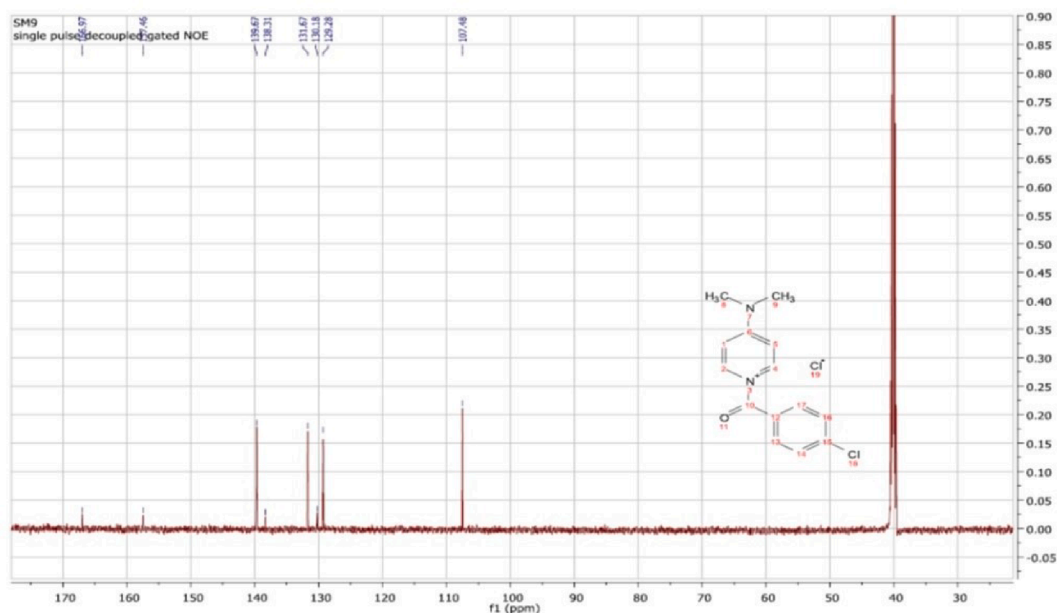


Fig. 1a. ^{13}C NMR spectrum of 1-(4-chlorobenzoyl)-4-(dimethylamino)pyridine-1-ium chloride (SM-9).

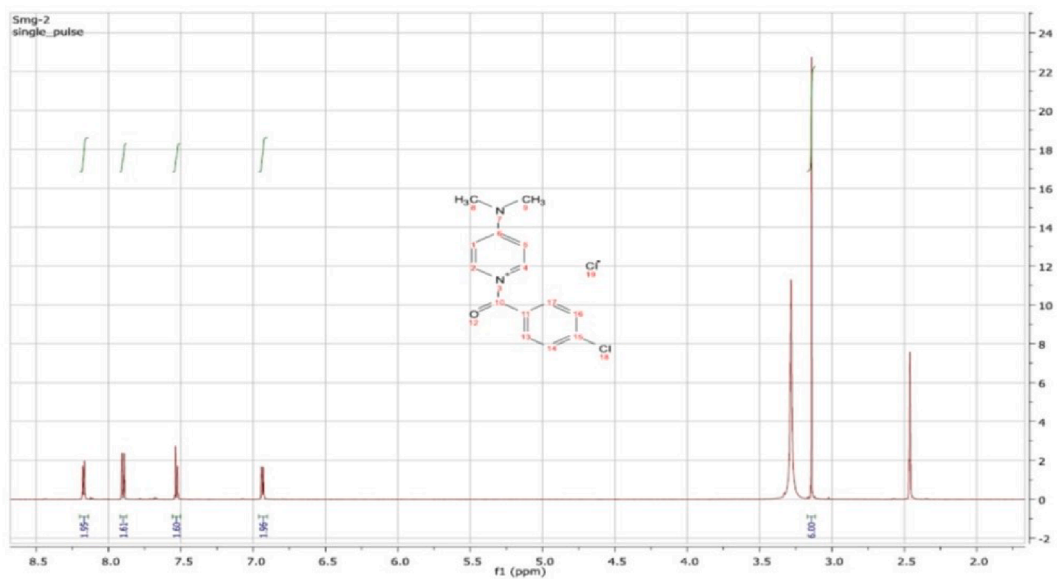


Fig. 1b. ^1H NMR spectrum of 1-(4-chlorobenzoyl)-4-(dimethylamino)pyridine-1-ium chloride (SM-9).

2019). This is the first study to report the adverse effects of the synthesized SM-9 compound on human colon cancer cells. In this study, we aimed to determine the safety profile of the SM-9 compound on human colon cancer cells.

2. Materials and Methods

2.1. Chemicals and reagents

Trypsin, antibiotic/antimitotic solution (100 \times), stabilized, 2',7'-dichlorodihydrofluorescein diacetate (DCFH-DA), MTT dye, and sodium chloride were purchased from Sigma-Aldrich (St. Louis, MI). Human apoptosis array C1 (Code: AAH-APO-1-2) was purchased from Ray Biotech. Fetal bovine serum and Dulbecco's modified Eagle's medium (DMEM)/Nutrient Mixture F-12 Ham were purchased from Gibco. All other chemicals such as 4-chlorobenzoyl chloride (1.1 eq), DMSO, and

ethyl alcohol were purchased from the local market of Riyadh, Saudi Arabia.

2.2. Synthesis of a new chemical material

2.2.1. Synthesis of the new chemical compound SM-9

4-Chlorobenzoyl chloride (1.1 eq) was added to a solution of 4-dimethylaminopyridine (1 eq) in toluene, followed by stirring at 80 $^{\circ}\text{C}$ for 24 h. The separation of viscous liquid from the initially obtained clear and homogeneous mixture of 4-dimethylaminopyridine and 4-chlorobenzoyl chloride in toluene marked the completion of the reaction. Extraction was used to separate the product from the unreacted starting materials and solvent. Finally, all volatile organic compounds were removed from the residue by drying it under pressure (Fig. 1a, Fig. 1b).

Table 1

Half-maximal inhibitory concentration (IC₅₀) and other concentrations of the SM-9 compound applied on the HCT-116 cells.

24-h IC ₅₀ = 400-µg/ml SM-9 compound	
Percentage (%)	Concentrations (µg/ml)
1/8 of IC ₅₀	50
1/2 of IC ₅₀	100
2/3 of IC ₅₀	266

2.2.2. Characterization of the SM-9 compound

1-(4-Chlorobenzoyl)-4-(dimethylamino) pyridin-1-ium chloride was characterized as follows: MP 83–84 °C, ¹H NMR (DMSO, 400 MHz,) δ 8.17 (d, 2H), 7.91 (d, 2H), 7.54 (d, 2H), 6.94 (d, 2H), 3.14 (s, 6H). ¹³C NMR (DMSO, 100 MHz,) δ 166.9, 157.4, 139.6, 138.3, 131.6, 130.1, 129.2, 107.4, 40.; IR (ν_{max} cm⁻¹) 3129 (C–H, sp²), 1559–1469 (C=C), 1163 (C–N), and 1080 (C–O) (Fig. 1a, Fig. 1b).

2.3. Cell culture

Colon cancer (HCT-116) cell lines were bought from ATCC (American Type Culture Collection, Manassas, VA). The cells were maintained in DMEM with fetal bovine serum (10 %) and antibiotics, namely penicillin and streptomycin (10,000 U/ml), in a CO₂ incubator (5 %) at 37 °C.

2.4. Exposure to the SM-9 compound

The HCT-116 cells were subcultured for 24 h before exposure to the SM-9 compound. Stock suspension of the SM-9 compound (50 mg/ml DMSO) was prepared in slightly warm DMSO. The stock suspension of the drug was diluted according to the experimental concentration. In this experiment, we applied different concentrations of the compound (control, solvent control, 50, 100, 200, 300, 400, and 500 µg/ml) to determine its toxicity level. The untreated cells were used as the controls.

2.5. MTT assay

The cell viability of the HCT-116 cells was determined using the MTT test (Alarifi et al., 2015; Alarifi et al., 2017) after exposure to various concentrations of the compounds (control, solvent control, 50, 100, 200, 300, 400, and 500 µg/ml) for 24 h. After adding MTT dye (0.05 mg/ml) to each well, the plate was incubated for 4 h. Formazan crystal was solubilized in organic solvent after 15-min incubation at room temperature. The optical density of the culture plate was measured at 570 nm using a microplate reader (BioTek Instruments, Winooski, VT) with the Gen5 software (version 1.09).

The 24-h half-maximal inhibitory concentration (IC₅₀) of the SM-9 compound was determined on the basis of the MTT test result. On the basis of the 24-h IC₅₀ of the SM-9 compound, we fixed 3 sublethal concentrations for further experiment (Table 1).

2.6. Evaluation of ROS generation

After the exposure of the HCT-116 cells to the SM-9 compound (50, 100, and 266 µg/ml), the ROS levels were evaluated using the method of Ali et al. (2021). The cells (3 × 10⁴) were subcultured in a black-bottom culture plate (96 wells) and kept in a CO₂ incubator at 37 °C for 24 h. Later, the culture plates treated with the compound were incubated for 24 h. After 24 h, DCFH-DA (10 µM) was mixed in each well for 35 min at 37 °C. After incubation, the plate was washed with chilled PBS, and the fluorescence intensity was evaluated at 485 nm excitation and 520-nm emissions using a microplate reader with the Gen5 software (version 1.09; Bio-Tek Instruments, Winooski, VT). The results were expressed as fluorescence intensity percentages in comparison with those of the

Table 2

List of primer sequences of the apoptotic genes.

Gene	Primer F sequence	Primer R sequence
Bcl2	ATGTGTGTGGAGAGCGTCAA	GGGCCGTACAGTTCACAAA
Bax	TGAAGCGACTGATGTCCTG	GGGCCGTACAGTTCACAAA
TP53	TGAAGCGACTGATGTCCTG	CAAAGATGGTCACGGTCTGC
GAPDH	GGGAAGCTTGTCAATCAATGG	GAGATGATGACCCTTTTGGC

controls. A separate set of experiments were performed to assess the generation of ROS through a qualitative analysis method (Ali et al., 2021).

2.7. Protein array for detecting apoptosis

To determine the mechanism of apoptosis induced by the SM-9 compound, a protein array (Human Apoptosis Array C1, code: AAH-APO-1-2; Ray Biotech) was applied to identify the proteins related to apoptosis. The HCT-116 cells were exposed to the SM-9 compound (0, 50, 100, and 266 µg/ml) for 24 h. The proteins (200 µg) extracted from the control and exposed cells were incubated for 5 h with the human apoptosis antibody array. The apoptosis protein array membranes were scanned using a Biorad Chemi Doc XRS + Imaging System (Tide Mill Road, Units 3, 4). The obtained data were analyzed using the Image Lab software (Biorad Chemi Doc XRS +), and the protein signal intensities of all samples were assessed in accordance with the manufacturer's instructions (code: AAH-APO-1-2; Ray Biotech).

2.8. Gene expression

2.8.1. RNA isolation and cDNA synthesis

The fresh cell lysates of the control and SM-9 compound-treated HCT cells were prepared. In accordance with the protocol of the manufacturer of the RNeasy Mini Kit (Qiagen, Germany), we isolated total RNA from the cells. The quality of the RNA was determined using a NanoDrop 2000c spectrophotometer (Thermo Fisher Scientific). We synthesized the cDNA using a cDNA synthesis kit (BioRad) in accordance with the manufacturer's instructions.

2.8.2. Reverse transcription-polymerase chain reaction

The expressions of the apoptotic genes such as Bax, Bcl2, and Tp53 in the HCT cells were analyzed using the PowerUp SYBR Green Master Mix (Applied Biosystems) and LightCycler 480 (Roche, Basel, Switzerland) in accordance with the manufacturer's instructions. We performed all the experiments in duplicate. The primers shown in Table 2 were used for the apoptotic gene expressions in the SM-9 compound-treated HCT cells. GAPDH was used as a housekeeping gene, and the fold change in relative quantification was determined using the formula $2^{-\Delta\Delta Ct}$.

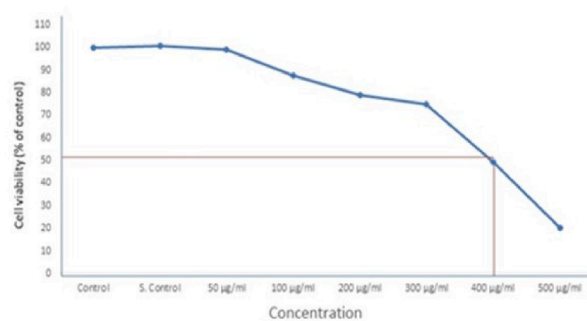


Fig. 2. Determination the IC₅₀ 24 h for SM-9 drug in HCT-116 Cells Each value represents the mean ± SE of five experiments. *n* = 3, **p* < 0.05* **p* < 0.01 vs. control.

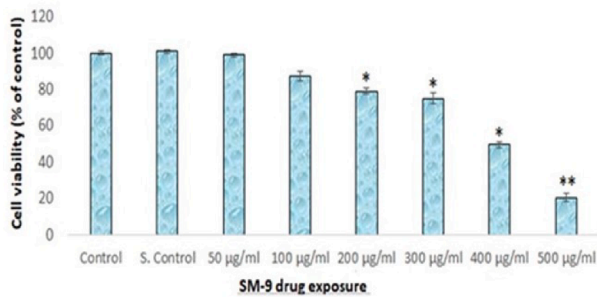


Fig. 3. Cytotoxicity of SM-9 drug in HCT-116 Cells over 24 h, as evaluated by MTT as says. Each value represents the mean ± SE of five experiments. n = 3, *p < 0.05* **p < 0.01 vs. control.

2.9. Statistical analysis

The results were analyzed using the SPSS 26.0 software (IBM) and expressed as mean ± standard deviation (SD). The following p values were considered statistically significant: *p < 0.05 and **p < 0.01.

3. Results

3.1. Determination the IC₅₀ value of the SM-9 compound

We calculated the median inhibitory concentration (IC₅₀ for 24 h) of the SM-9 compound in the HCT-116 cells on the basis of the MTT test results by using the OrigenPro 8.5 program. The IC₅₀ value of the SM-9 compound applied on the HCT-116 cells was 400 µg/ml (Fig. 2, Table 1).

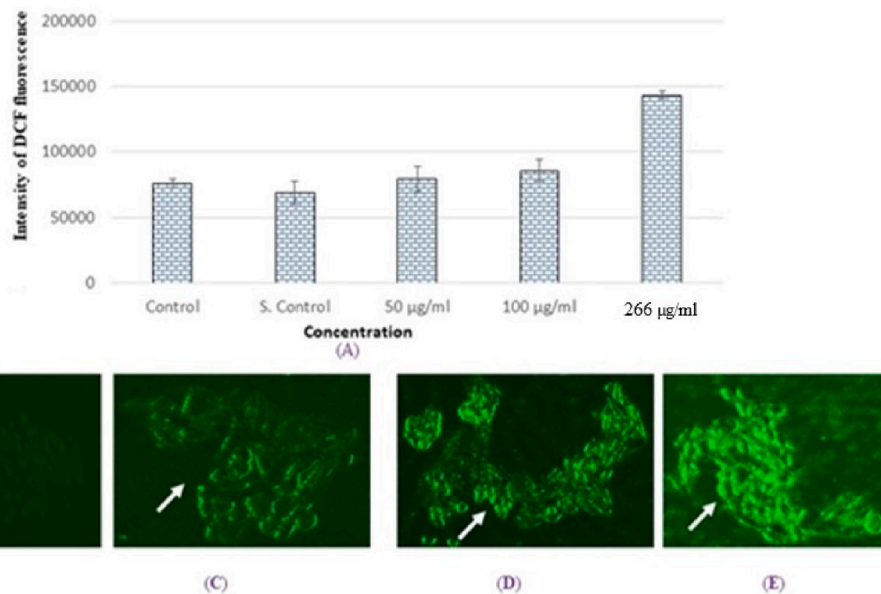


Fig. 4. Production of intracellular ROS in HCT cells for 24 h due to SM-9 drugs exposure (A). Percent of DCF fluorescence intensity and generation green fluorescence in HCT cells for 24 h (B). Control HCT cells (C). HCT cells at 500 µg/ml (D). HCT cells at 100 µg/ml (E). HCT cells at 266 µg/ml Each value represents the mean *SE of three experiments. *p < 0.05 vs Control. Arrow indicate green fluorescence intensity in cell as marker of ROS generation.

	A	B	C	D	E	F	G	H	I	J	K	L	M	N
1	Pos	Pos	Neg	Neg	Blank	Blank	bad	bax	bcl-2	bcl-w	BID	BIM	Caspase3	caspase8
2	Pos	Pos	Neg	Neg	Blank	Blank	bad	bax	bcl-2	bcl-w	BID	BIM	Caspase3	caspase8
3	CD40	CD40L	ciAP-2	cytoC	DR6	Fas	FasL	Blank	HSP27	HSP60	HSP70	HTRA	IGF-I	IGF-II
4	CD40	CD40L	ciAP-2	cytoC	DR6	Fas	FasL	Blank	HSP27	HSP60	HSP70	HTRA	IGF-I	IGF-II
5	IGFBP-1	IGFBP-2	IGFBP-3	IGFBP-4	IGFBP-5	IGFBP-6	IGF-1sR	livin	p21	p27	p53	SMAC	Survivin	sTNF-R1
6	IGFBP-1	IGFBP-2	IGFBP-3	IGFBP-4	IGFBP-5	IGFBP-6	IGF-1sR	livin	p21	p27	p53	SMAC	Survivin	sTNF-R1
7	sTNF-R2	TNF-alpha	TNF-beta	TRAILR-1	TRAILR-2	TRAILR-3	TRAILR-4	XIAP	Blank	Blank	Neg	Neg	Neg	Pos
8	sTNF-R2	TNF-alpha	TNF-beta	TRAILR-1	TRAILR-2	TRAILR-3	TRAILR-4	XIAP	Blank	Blank	Neg	Neg	Neg	Pos

Blank: Blank spot
 Neg: Negative control spot
 Pos: Positive control spot

Fig. 5a. Analysis of apoptosis-related in HCT-116 cells due to SM-9 compound exposure. Template showing the location of apoptosis-related antibodies spotted on the Human Apoptosis Array C1 kit.

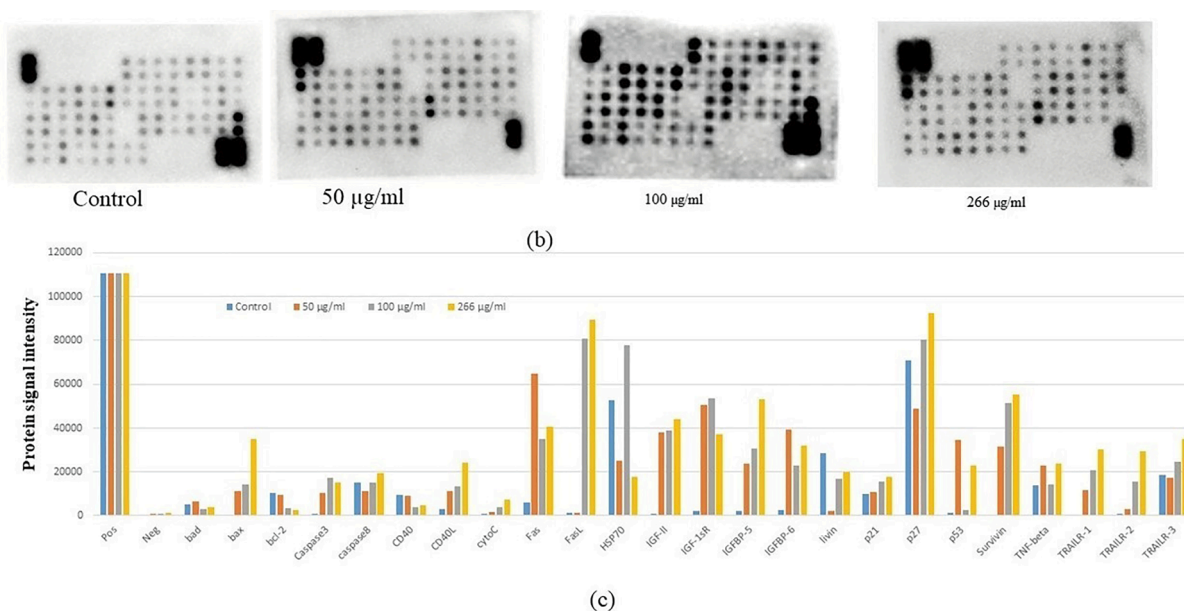


Fig. 5b-c. (b) Equal quantity protein extracts from control treated HCT-116 cells were analyzed using the antibody array. The chemiluminescent intensities were quantified by densitometry. A Positive control was used normalize the results from different membranes. (c) Representative bar graph of the apoptotic unregulated and downregulated protein.

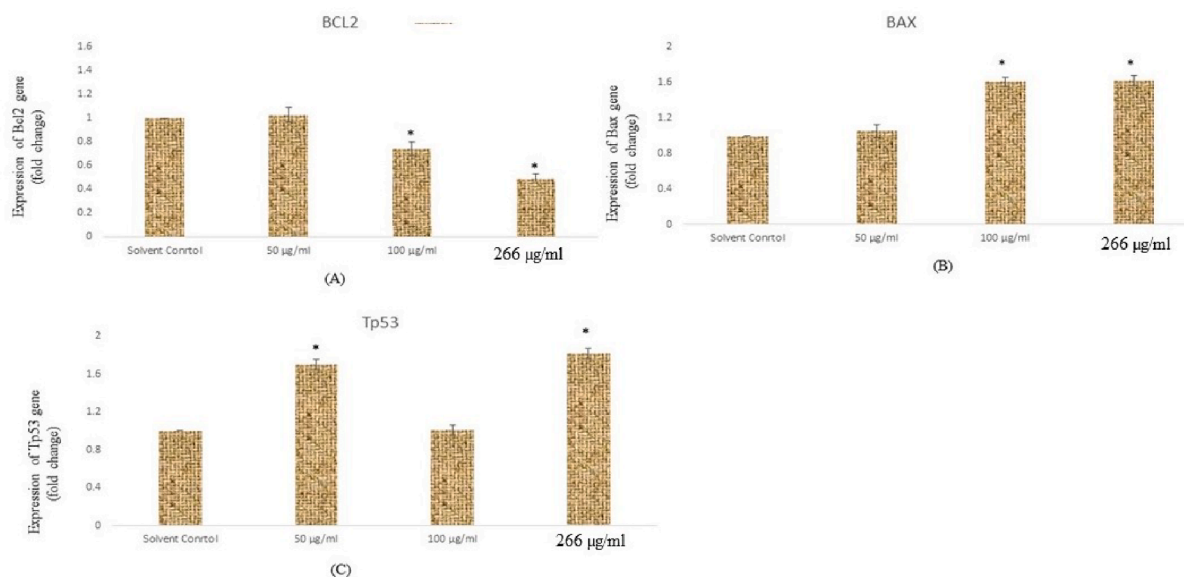


Fig. 6. Expressions of apoptotic genes in HCT cells exposed to SM-9 drug for 24 h. Expression of (A) Bcl2 (B) Bax, (C) p53, gene in HCT cells for 24 h. Results are expressed in average \pm SD of triplicate experiments. * $p < 0.05$ vs. solvent control.

3.2. Cytotoxicity

The cytotoxicity of the SM-9 compound in the HCT cells was determined using an MTT assay. The SM-9 compound induced toxicity in a dose-dependent manner. The HCT cells treated with SM-9 had higher cell death rates than the untreated cells. The SM-9 compound exhibited a significant toxic effect on the HCT cells at 500 µg/ml (Fig. 3).

3.3. Intracellular ROS

The ROS production increased as exposure to the compound increased, and we observed a high intensity of green fluorescence with 266-µg/ml SM-9 compound (Fig. 4A, E). In this study, we determined

the intracellular ROS production by measuring the DCF intensities in the SM-9 compound-exposed cells (Fig. 4). The maximum ROS production was found at a SM-9 concentration of 266 µg/ml (Fig. 4A).

3.4. Apoptotic protein expressions

After the treatment of the HCT cells with various SM-9 concentrations for 24 h, a team member analyzed the specific proteins related to apoptosis and toxicity using a human apoptosis protein array (Fig. 5a-c). As indicated in Fig. 5, we found changes in the apoptotic proteins. Many proteins were downregulated, including Bad, Bcl2, and CD40, and upregulated, including Bax, Caspase-3, Caspase-8, CD40L, cytochrome C, Fas, Fas ligand, Hsp70, HTRA, IGF-1sr, IGF-2, IGFBP5, IGFBP6, livin,

P21, P27, P53, survivin, TNF- β , TNFR-II, TRAIL-1, TRAIL-2, and TRAIL-3, depending on its role in the apoptosis pathway (Fig. 5).

3.5. Apoptotic gene expressions in the HCT-116 cells

To confirm the mechanism of the toxicity induced by the SM-9 compounds in HCT-116 cells, we determined the expression levels of specific genes such *Bcl2*, *Bax*, and *TP53*. Reverse transcription-polymerase chain reaction (RT-PCR) analysis was performed to determine the expression levels of the apoptotic genes (e.g., *Bcl2*, *Bax*, and *p53*) in the HCT cells. Higher gene expression levels were observed with SM-9 compound treatment at 200 $\mu\text{g/ml}$ after 24 h of exposure (Fig. 6A–C). The *p53* gene expression was downregulated in the cells with exposure to the SM-9 compound at 100 $\mu\text{g/ml}$ but upregulated at 50 and 266 $\mu\text{g/ml}$ (Fig. 6C). Other apoptotic genes such as *Bcl2* and *Bax* were expressed in the HCT cells (Fig. 6A, B).

4. Discussion

The production of novel chemical compounds has increased significantly in recent years on a global scale, and it is fascinating to use this technology in the pharmaceutical industry for the benefit of human health. However, the significant and concurrent consequence of the increasing use of chemicals could be detrimental to the ecosystem, as people may not be aware of the risk of drug exposure or the different ways chemicals can infiltrate biological systems (Yang et al., 2012). This study examined the biological reactions that occurred when the SM-9 compound was exposed to human colon cancer (HCT-116) cells.

We found that the SM-9 compound caused a dose-dependent toxicity, ROS production, and apoptosis in HCT-116 cells. The finding that HCT-116 cells are susceptible to SM-9 is more significant. The bioactivity of the SM-9 compound may be due to the presence of the 1-(4-chlorobenzoyl)-4-(dimethylamino) group, warranting further analysis. The ROS production level was higher in the HCT-116 cells after exposure to the maximum concentration of the SM-9 compound, demonstrating that a higher SM-9 dose will be more effective in minimizing the growth of cancer cells. ROS plays a major role in various cellular mechanisms such as cell cycle, cell proliferation, and gene expression, and, ultimately, stops the mechanism of cell growth or cell death (Almutairi et al., 2020). Our investigation revealed that SM-9 was advantageous for use as an anticancer medication and sensitive to HCT-116 cells. The RT-PCR analysis performed to assess the apoptotic potential of the SM-9 compound in these cells revealed that higher SM-9 concentrations had a greater apoptotic effect. The correlation between the induction of cytotoxicity, oxidative stress, and apoptotic gene expression indicated that exposure to a higher dose of SM-9 chemical was more effective. In the HCT-116 cells, all the results proved the anticancer capabilities of the SM-9 compound. The untreated HCT-116 cells showed the decreased protein signal fluorescence intensity of various proteins such as bad, bax, bcl2, p53, p21, Hsp70, p27, TRAIL-1, TRAIL-2, TRAIL-3, and TNF β compared with the SM-9 compound-treated HCT-116 cells. The current finding indicated that the effect of the SM-9 compound inhibited the bad and bcl2 signaling pathways in the HCT-116 cells. These findings suggest that bad and bcl2 regulations could be chunked using the SM-9 compound. The results show that both types of apoptotic pathways may be involved in the induction of apoptosis in HCT-116 cells by upregulating caspase-8 and p53 expression levels and reducing bad and bcl2 levels in the cytoplasm and nucleus. The concerns about the mitochondrial-intrinsic actions indicated by mRNA and the upregulation of the p53, bax, and cytochrome *c* expression levels could elicit mitochondrial damage and dysfunction by enhancing caspase-8 levels. Protein arrays are useful because they can provide a map of known cell apoptotic and signaling proteins. Protein arrays have shown a unique ability to analyze signaling pathways using small numbers of cultured cells or cells (Grubb et al., 2003). By using this approach, untreated and treated HCT-116 cells of protein lysate are arrayed onto nitrocellulose-

coated slides. The main technological components of this method offer unique advantages for detecting multi-protein expressions.

In this paper, a useful methodology for the synthesis of a novel chemical compound is described. The results show that the SM-9 compound has high efficacy and should be given particular consideration in anticancer treatments. Furthermore, this finding demonstrates that the SM-9 compound killed the colon cancer cells and induced apoptosis by activating various proteins and genes such as *caspase-8*, *p53*, *NF- β* , and *bax*. The results established that the SM-9 compound may be applied as a medicinal drug alone or in combination with other chemotherapeutics for different types of cancer cells. In the future, we will investigate the mechanism of the toxicity of the SM-9 compound in *in vivo* experiments.

Declaration of competing interest

The authors declare that they have no known competing financial interests or personal relationships that could have appeared to influence the work reported in this paper.

Acknowledgments

The authors extend their appreciation to the Deputyship for Research and Innovation, “Ministry of Education,” in Saudi Arabia for funding this research (IFKSUOR3-243-4).

Appendix A. Supplementary material

Associated with this article are the 1H and 13C NMR spectra of the SM-9 compound.

Supplementary data to this article can be found online at <https://doi.org/10.1016/j.jksus.2024.103101>.

References

- Alarifi, S., Ali, D., Alkahtani, S., 2015. Nanoalumina induces apoptosis by impairing antioxidant enzyme systems in human hepatocarcinoma cells. *Int. J. Nanomed.* 10 (1), 3751–3760.
- Alarifi, S., Ali, D., Alkahtani, S., 2017. Oxidative stress-induced DNA damage by manganese dioxide nanoparticles in human neuronal cells. *Biomed. Res. Int.* 2017, 5478790.
- Albalawi, A.H., El-Sayed, W.S., Aljuhani, A., Almutairi, S.M., Rezki, R., Aouad, M.R., et al., 2018. Microwave-assisted synthesis of some potential bioactive imidazolium-based room-temperature ionic liquids. *Molecules* 23, 1727.
- Ali, H., Yadav, Y.K., Ali, D., Kumar, G., Alarifi, S., 2023. Biosynthesis and characterization of cobalt nanoparticles using combination of different plants and their antimicrobial activity. *Biosci. Rep.* 43(7), BSR20230151.
- Ali, D., Ibrahim, K.E., Hussain, S.A., Abdel-Daim, M.M., 2021. Role of ROS generation in acute genotoxicity of azoxystrobin fungicide on freshwater snail *Lymnaea luteola* L. *Environ. Sci. Pollut.* 28, 5566–5574.
- Almutairi, B., Albahser, G., Almeer, R., Alyami, N.M., Almukhlafi, H., Yaseen, K.N., et al., 2020. Investigation of cytotoxicity apoptotic and inflammatory responses of biosynthesized zinc oxide nanoparticles from *ocimum sanctum* linn in human skin keratinocyte (HaCat) and human lung epithelial (A549) cells. *Oxid. Med. Cel Longev.* 2020, 1835475.
- Almutairi, B., Ali, D., Yaseen, K.N., Alothman, N.S., Alyami, N., Almukhlafi, H., et al., 2021. Mechanisms of apoptotic cell death by stainless steel nanoparticle through reactive oxygen species and caspase-3 activities on human liver cells. *Front. Mol. Biosci.* 8, 729590.
- Bardelčíková, A., Soltys, J., Mojzís, J., 2023. Oxidative stress, inflammation and colorectal cancer: an overview. *Antioxidants (basel)*. 12 (4), 901.
- El-Hajjaji, F., Messali, M., Martínez de Yuso, M.V., Rodríguez-Castellón, E., Almutairi, S., Bandoz, T.J., et al., 2019. Effect of 1-(3-phenoxypropyl) pyridazin-1-ium bromide on steel corrosion inhibition in acidic medium. *J. Colloid Interface Sci.* 541, 418–424.
- El-Sayed, I.H., Huang, X., El-Sayed, M.A., 2005. Surface plasmon resonance scattering and absorption of anti-EGFR antibody conjugated gold nanoparticles in cancer diagnostics: applications in oral cancer. *Nano Lett.* 5, 829–834.
- Grubb, R.L., Calvert, V.S., Wulfskuhle, J.D., Pawletz, C.P., Linehan, W.M., Phillips, J.L., et al., 2003. Signal pathway profiling of prostate cancer using reverse phase protein microarrays. *Proteomics* 3 (11), 2142–2146.
- Hansford, R.G., Hogue, B.A., Mildaziene, V., 1997. Dependence of H2O2 formation by rat heart mitochondria on substrate availability and donor age. *J. Bioenerg. Biomembr.* 29, 89–95.
- Schumacker, P.T., Gillespie, M.N., Nakahira, K., Choi, A.M.K., Crouser, E.D., Piantadosi, C.A., et al., 2014. Mitochondria in lung biology and pathology: more than just a powerhouse. *Am. J. Physiol. Lung Cell Mol. Physiol.* 306 (11) L962-L974.

- Su, L.J., Zhang, J.H., Gomez, H., Murugan, R., Hong, X., Xu, D., Jiang, F., Peng, Z.Y., 2019. Reactive Oxygen Species-Induced Lipid Peroxidation in Apoptosis, Autophagy, and Ferroptosis. *Oxid. Med. Cell. Longev.* 2019, 5080843.
- Titi, A., Almutairi, S.M., Alrefaei, A.F., Manoharadas, S., Alqurashy, B.A., Sahu, P.K., et al., 2020. Novel phenethylimidazolium based ionic liquids: design, microwave synthesis, in-silico, modeling and biological evaluation studies. *J. Mol. Liq.* 315, 113778.
- Titi, A., Almutairi, S.M., Touzani, R., Messali, M., Tillard, M., Hammout, B., et al., 2021. New mixed pyrazole-diamine/Ni (II) complex, crystal structure, physicochemical, thermal and antibacterial investigation. *J. Mol. Struct.* 1236, 130304.
- Tu, Y., Quan, T., 2016. Oxidative Stress and Human Skin Connective Tissue Aging. *Cosmetics* 3, 28.
- Yang, H., Xing, L., Zhou, M.-G., 2012. Network pharmacological research of volatile oil from Zhike Chuanbei Pipa Dropping Pills in treatment of airway inflammation. *Chin. Tradit. Herb. Drugs.* 43, 1129–1135.